Pore-Level Modeling of Carbon Dioxide Sequestration in Brine Fields

M. Ferer, (mferer@wvu.edu) Department of Physics, West Virginia University, Morgantown, WV 26506-6315, Grant S. Bromhal, (bromhal@netl.doe.gov) US DOE, National Energy Technology Laboratory, Morgantown, WV 26507-0880; and Duane H. Smith, (dsmith@netl.doe.gov) US DOE, National Energy Technology Laboratory, Morgantown, WV 26507-0880 & Department of Physics, West Virginia University.

Underground injection of gas is a common practice in the oil and gas industry. Injection into deep, brine-saturated formations is a commercially proven method of sequestering CO_2 . However, it has long been known that displacement of a connate fluid by a less viscous fluid produces unstable displacement fronts with significant fingering. This fingering allows only a small fraction of the pore volume of a brine-saturated formation to be available for sequestration, while providing a large interfacial region between the carbon dioxide and the brine. A better understanding of the fluid displacement process should lead to reduced capital and operating costs for CO_2 sequestration in brine fields. The interfacial length will provide information to study the extent of dissolution of CO_2 in the brine as well as the extent of possible hydrate formation. By studying the flow for several viscosity ratios, the effect of polymeric viscosifiers can be evaluated.

We have developed a pore-level model of the immiscible injection of CO_2 (a non-wetting fluid) into a porous medium saturated with brine (a wetting fluid). This model incorporates a distribution of different 'pore-throat' radii , the wettability of the formation (i.e. the gas-liquid-solid contact angle, the interfacial tension between the fluids, the fluid viscosities, and all other parameters that appear in the capillary number. The computer code for the model maintains a constant injection to within a few per cent.

The model has been used with experimental values of interfacial tensions and a range of possible viscosities, to study the injection of carbon dioxide into brine-saturated porous media, at high pressures. Results are presented for saturations and fingering patterns for a range of capillary numbers and viscosities.

I. Introduction

Flow in porous media is a subject of scientific and engineering interest for a number of reasons. For half a century, it has been believed that flow in porous media is a compact (i.e. Euclidean) process whereby the interface advances linearly with the total amount of the fluid as predicted by a Darcy's law treatment using saturation-dependent relative permeabilities.[1]-[5] In the last fifteen years, it has been appreciated that flow in porous media is fractal in certain well-defined limits.[6]-[9] The flow is known to be described by self-similar diffusion-limited-aggregation (DLA) fractals in the limit of zero viscosity ratio, $M = \mu_I / \mu_D = 0$ (i.e. where the injected fluid has zero viscosity and the displaced fluid has finite viscosity). [6]-[8],[10]-[12] The flow is known to be described by self-similar invasion percolation fractals in the limit of zero capillary number, $N_C = \mu_D V / \sigma \cos\theta = 0$, where viscous drag forces

(viscosity of the displaced fluid times average fluid velocity) are zero, while the capillary forces (proportional to interfacial tension, σ, times sine of the contact angle θ) are finite.

Diffusion Limited Aggregation (DLA) was originally introduced to describe colloidal aggregation.[13] Soon, it was appreciated that because the continuum versions of both DLA and viscous fingering are both governed by Laplace's Equation, both should provide equivalent displacement patterns in the limit of zero viscosity ratio.[14] Indeed, evidence from both experiment and modeling showed that not only were the DLA and viscous fingering patterns visually similar but they also had the same fractal character.[6]-[9] ,[11],[12],[15]-[19]

Invasion Percolation was proposed as a model of immiscible drainage (where a non-wetting fluid is injected into a medium saturated with a wetting fluid), in the limit of zero injection velocity, i.e. at zero capillary number. [7]-[9],[20] In Invasion Percolation, only the largest throat (with the smallest capillary pressure) on the interface is invaded by the injected, non-wetting fluid. In this Invasion Percolation rule, it is assumed that wetting fluid will be displaced towards the outlet. However, in two dimensions, one may need to include trapping effects where a blob of the wetting fluid cannot reach the outlet because it is surrounded by non-wetting fluid. The patterns of injected fluid from Invasion Percolation with trapping (IPwt) have been observed to have a fractal character with a fractal dimension $D \approx 1.82$.[7]-[9],[20] Experiments have shown that patterns of drainage at small capillary number ($N_{Ca} = 10^{-5}$) are visually similar to patterns from IPwt and that they have the same fractal dimension, $D \approx 1.84$, as IPwt.[21]

Recently, we have shown that our model produces results which agree with both DLA (in the limit of very large viscosity ratio) and with IPwt (in the limit of very small capillary number).[22] Having demonstrated the validity of our model in these two very different limits, coupled with the physicality of the model and the excellent consistency with fluid conservation, we are be confident in extending our studies to the physically relevant intermediate regime, where the limiting models (DLA and IPwt) are not valid.

II. Objectives

We have used our computer model, as described in Section III, to study the injection of carbon dioxide into a brine saturated reservoir. In our modeling, we used typical experimental values of surface tension and viscosity for carbon dioxide at high pressures , $\sigma = 21$ dynes/cm, $\mu \approx 0.05$ cp (viscosity ratio M=0.05) and larger.[23],[24] We assumed a water-wet porous medium, i.e. a contact angle $\theta = 0^o$. We assumed a size scale for the porous medium where the typical pores are 100μm apart (i.e. the length scales in our model is $\ell = 100\mu m$). For our model, this would give a smallest capillary pressure of 7500 dynes/cm^2 . Although this size scale would significantly affect the pressure necessary to inject the carbon dioxide, the saturations should be more directly affected by variations in capillary number than by the size scale of the porous medium.

In section IV, we present results for the saturation profiles and fingering patterns from a range of capillary numbers for model systems with 2700 pore bodies. Surprisingly for these systems, the saturation's are nearly independent of capillary number. The fingering patterns

show that the saturation's are consistent with IPwt at small capillary numbers; for this small viscosity ratio, the fingering changes from IPwt-like to DLA-like as the capillary number increases. Both fingering models (IPwt and DLA) yield small CO_2 saturations. For larger viscosity ratios, we show that the saturations increase with capillary number as expected.

III. Approach - Description of the Model

The pore-level model is intended to incorporate, as realistically as possible, both the capillary pressure that tends to block the invasion of narrow throats and the viscous pressure drop in a flowing fluid. The two-dimensional model porous medium is a diamond lattice, Fig.1, which consists of pore bodies of volume, ℓ^3, at the lattice sites and throats connecting the pore bodies which are of length, ℓ, and have a randomly chosen cross-sectional area between 0 and ℓ^2. Compared to several models reported in the recent literature, we believe that our model should be both more general and more flexible, in part because both the throats and the pore bodies have finite volume in comparison with i) refs. [6] and [25], where the throats contain zero volume of fluid, and ii) refs. [26]-[28], where the pore bodies have zero volume. Furthermore, in our model, the volumes of both the pore bodies and throats can be set as desired. In this sense the work of Periera is closer to our model, but this work focuses on three-phase flows at constant pressure.[29] Of course all of these models include the essential features of random capillary pressures blocking the narrowest throats and a random conductivity depending on a given viscosity ratio.

III.A. Capillary Pressure

When the interface has entered one of the pore throats, the radius of curvature, R, of the meniscus is fixed by contact angle, θ, and the radius of the pore throat, r ;

$$R = r/\cos\theta \quad . \tag{1}$$

Therefore, the pressure drop across the meniscus is fixed at the capillary pressure

$$P_{cap}(R) = \frac{2\ \sigma\ \cos\theta}{r} \quad , \tag{2}$$

where σ is the surface tension. Thus the flow velocity is given by the throat conductance times the total pressure drop across the throat; see Fig. (2),

$$q = g_{throat}\ (P_{nw} - P_w - P_{cap}). \tag{3a}$$

In the model the transmissibility (conductance) of the throat is given by

$$g_{throat} = g^* \frac{(A_{throat}^2/\ell^4)}{(x + (1-x)\ M)} \tag{3b}$$

where A_{throat} is the cross-sectional area of the throat, x is the fraction of the throat of length ℓ which is filled with defending fluid, and M is the ratio of the non-wetting, invading fluid's (CO_2) viscosity to that of the wetting, defending fluid (brine), $M = \mu_{nw} / \mu_w$. (Note: this definition

of

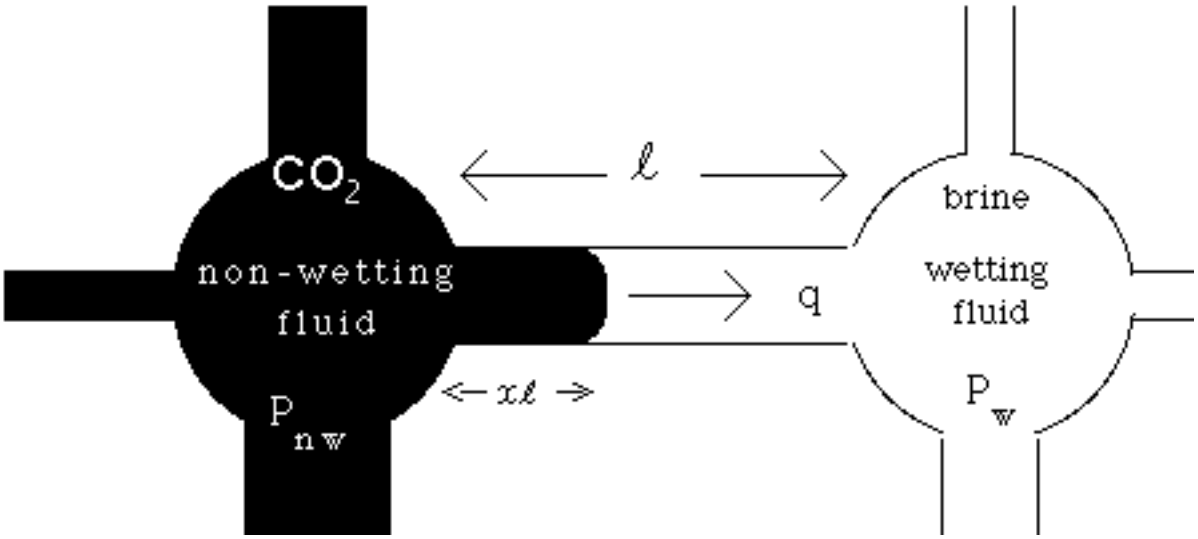

Figure 1

shows the CO_2 displacing the brine with volume flow velocity $q_{throat} = g_{throat} (P_{nw} - P_w - P_{cap})$. of course if $P_{nw} - P_w < P_{cap}$ the CO_2 retreats and the brine re-occupies the throat.

M agrees with the convention of Lenormand [6], but it is the inverse of the convention used in our earlier papers on miscible, unstable flow [15]-[18].) The quantity, g*, carries all the dimensionality of g_{throat}

$$g^* = \ell^3 / (8 \pi \mu_w) \qquad (4)$$

Many of our results for the flow velocity will presented in terms of $q^* = q/g^*$, which is independent of the particular value of the viscosity of the wetting fluid. From Eq. (3a), the non-wetting fluid advances if the pressure difference between the pore filled with CO_2 (non-wetting fluid) and the pore filled with brine (wetting fluid) exceeds the capillary pressure. Otherwise the CO_2 will retreat.

Naive use of Eq. 2 causes a number of complications in the programming. These complications arise because of the blocking that occurs if the CO_2 fluid is at the entrance to a throat, Fig. 3; if the sign of the pressure drop ($P_{nw} - P_w$) is such that it would advance the non-brine but the magnitude of the pressure drop does not exceed the capillary pressure ($P_{nw} - P_w < P_{cap}$) , the interface remains stationary at the inlet of the throat. This will lead to very small time steps. If the CO_2 is close to the entrance of a narrow throat, which will likely be blocked to this invading fluid, a very small time step may be needed to advance the fluid to the entrance of the throat, but not into the throat. This makes a reliable control on the velocity difficult; as the inlet pressure is changed to maintain a constant flow the throat blockages will change requiring a complicated feedback loop connecting inlet pressure, flow velocity and throat blockages. A clever solution to these problems was suggested in refs. [26]-[28]; they argued that real throats would have a gradual decrease in cross-sectional area accompanied by a gradual increase in capillary pressure. Consistent with this work, we assume that the capillary pressure increases

from zero at the inlet to a throat of radius r and length ℓ to the value in Eq. 2 at the center of the throat. This dependence is given by the equation

$$P_{cap} = \frac{2\ \sigma\ \cos\theta}{r} \sin\left(\frac{\pi x}{\ell}\right), \qquad (5)$$

where x is still the distance along the throat from 0 to ℓ. Eq. (5) solves the problem of trying to advance a fluid into a blocked throat, because the inlet of a throat will never be blocked since it has zero capillary pressure. Furthermore, the feedback between blockage and the inlet pressure is removed, so that the constant velocity condition is easier to satisfy.

Implicit in this model, is the assumption that the pressure within a pore body is uniform. Assuming otherwise would require doing full fluid dynamics using the Navier-Stokes equation. This is inconsistent with the pore-level model approach and would severely limit the size of the model porous medium, given finite computer resources. Although, these idealizations (Eq. (5), etc.) may seem unphysical on a real microscopic scale, the model has a random distribution of conductances and correlated capillary pressures. Significantly, the pressure must exceed the randomly-distributed capillary pressures in Eq. 2 to pass through the throat; and the flow velocity (Eq. 3) has the correct dependence upon throat radius.

III.B. Finding the Pressure Field

Volume conservation of the incompressible fluid, dictates that the net volume flow q out of any pore body must be zero. Let us consider use of the above rules for the situation in Fig 2. In Fig. 2, the flow velocities, as directed out of the (i,j) pore body through the throats are

$$q_{i-2,i-1} = g_{i-2,i-1}\,(P_{i,j} - P_{i-2,i-2}) \qquad q_{i,j+1} = g_{i,j+1}\,(P_{i,j} - P_{i+2,j+2} - P_{cap,i,j+1})$$

$$q_{i-1,j} = g_{i-1,j}\,(P_{i,j} - P_{i-2,j} - P_{cap,i-1,j}) \qquad q_{i+1,j} = g_{i+1,j}\,(P_{i,j} - P_{i+2,j} - P_{cap,i+1,j}). \qquad (6a)$$

Requiring that the net flow out of pore body (i,j) be zero leads to the following equation for $P_{i,j}$:

$$(g_{i-2,i-1} + g_{i,j+1} + g_{i-1,j} + g_{i+1,j})P_{i,j} =$$
$$(g_{i-2,i-1}\,P_{i-2,i-2} + g_{i,j+1}\,P_{i+2,j+2} + g_{i-1,j}\,P_{i-2,j} + g_{i+1,j}\,P_{i+2,j}) + \qquad (6b)$$
$$(g_{i,j+1}\,P_{cap,i,j+1} + g_{i-1,j}\,P_{cap,i-1,j} + g_{i+1,j}\,P_{cap,i+1,j})$$

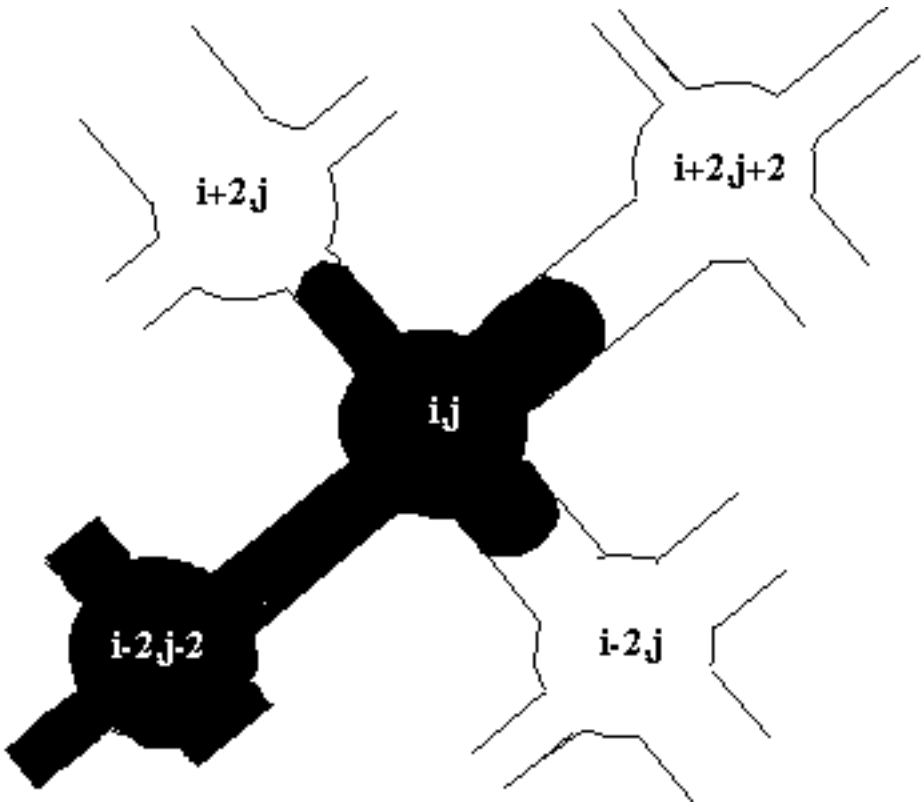

Figure 2
shows a possible occupation of adjacent pore-bodies. For this occupation, the flow velocities are given by Eq. (6a) and the pressure in the (i,j) pore body is given by Eq. (6b) (a specific realization of Eq. (7)).

Eq. (6b) is of the form

$$(\sum g)\, P_{i,j} = (\sum g\, P) + (\sum f\, g\, P_{cap}) \qquad (7)$$

where i) the factor f is zero if there is no meniscus in the throat; ii) the factor f is +1 if the pore body (i,j) is filled with non-wetting fluid (CO_2) and the connecting pore body is filled with wetting fluid (brine); iii) the factor f is -1 if the pore body (i,j) is filled with brine and the connecting pore body is filled with CO_2.

Once the location of the interface is known, the numerical value of the capillary pressure in each throat is known (zero, if the interface is neither in the throat nor at either inlet to the throat). Furthermore, for each pore body at (i,j), the values of the sums $(\sum g)$ and $(\sum f\, g\, P_{cap})$ can be calculated and stored; note that these sums are independent of the values of the pressures in the pore bodies. Then the program iterates (Eq. 7), determining the pressure field until stability is achieved where the residual is less than some small value; i.e. until

$$R = \sum (P_{new} - P_{old})^2 < \varepsilon, \qquad (8)$$

where ε is chosen to be small, e.g. $\varepsilon = 10^{-3}$. This value of ε is chosen to minimize run-time without seriously sacrificing mass-conservation. For example, in one of the typical sets of five runs presented in this paper, after an average of 77,000 time steps there was an average difference of less than 1% between the total volume of fluid injected into the medium and the total volume of fluid expelled from the medium.

To maintain a constant volume flow q_o, the flow velocity was determined for two estimates of the inlet pressure. Assuming a linear relationship between flow velocity and inlet pressure (consistent with Eq. 6a), the linear relationship would then predict an inlet pressure, P_o, to produce the desired volume flow, q_o.[28] If the two estimates of the inlet pressure are too close together, the prediction of P_o will be unreliable; on the other-hand, if the estimates of the inlet pressure are too far apart computer time will be wasted iterating Eq.7 to determine the different pressure fields for each. In practice, the difference between the two initial estimates needs to increase with capillary number. With a good choice of initial estimates, this procedure is very accurate; for a typical set of runs, the standard deviation from the average outlet flow velocity, q=50.4, represented an scatter of 0.007%.

III.C. Flow Rules

Once the pressure field has been determined, we can determine the interface advance through a time interval Δt. A throat is on the interface, if the pore body at one end contains some wetting fluid (it may be filled with wetting fluid) and if the pore body at the other end is fully invaded by non-wetting fluid (or was fully invaded and is not yet fully re-invaded by wetting fluid due to backflow). As discussed earlier, a time interval, Δt, needs to be chosen which is small enough that

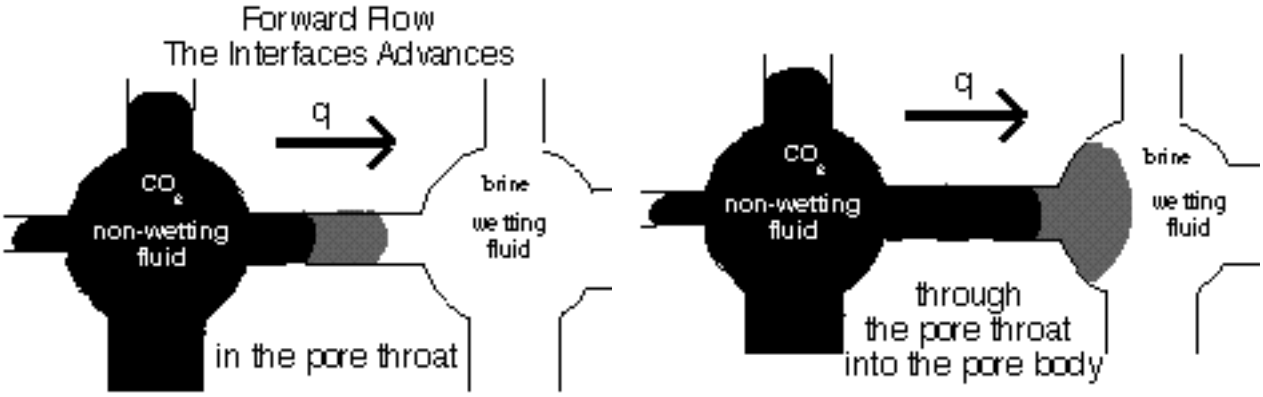

Figure 3 the CO_2 can advance within the pore throat (left-hand figure) or through the pore throat into the pore body (right-hand figure).

spurious local oscillations in the flow are avoided but not so small that the program run-time is unnecessarily long. For the cases discussed here, with large surface tension, the following prescription seems adequate. For all interfacial throats where the non-wetting fluid has yet to reach the midpoint of that throat, so that the capillary pressure is still increasing, the time interval is chosen so that the non-wetting fluid advances no more than 3.5% into any such throat. For all throats where the non-wetting fluid has advanced past the midpoint, so that the capillary pressure

is decreasing, the time step allows the interface to advance no further than 33% into any such throat. Having determined the interface and chosen the time step, we have attempted to make the flow rules as non-restrictive as possible.

Flow can increase the amount CO_2 within the pore throat (Fig. 3a), or through the pore throat into the pore body (Fig. 3b). Similarly, backflow can cause the interface to retreat within the pore throat (Fig. 4a) or through the pore throat into the pore body (Fig. 4b). If, during a time step, either type fluid over-fills a pore body, the excess is shared by the outflow throats. For these flow-rules, the throats are taken to be cylindrical with cross-sectional area A and length ℓ, consistent with refs. [26]-[28],[30] . The variation in the capillary pressure, Eq. (5), can be assumed to results from variations in contact angle. Again, this aspect of dubious microscopic physicality does not affect the basic feature of the model that the pressure drop across any throat must exceed the capillary pressure of that cylindrical throat, Eq. (2), for the non-wetting fluid to advance through the throat.

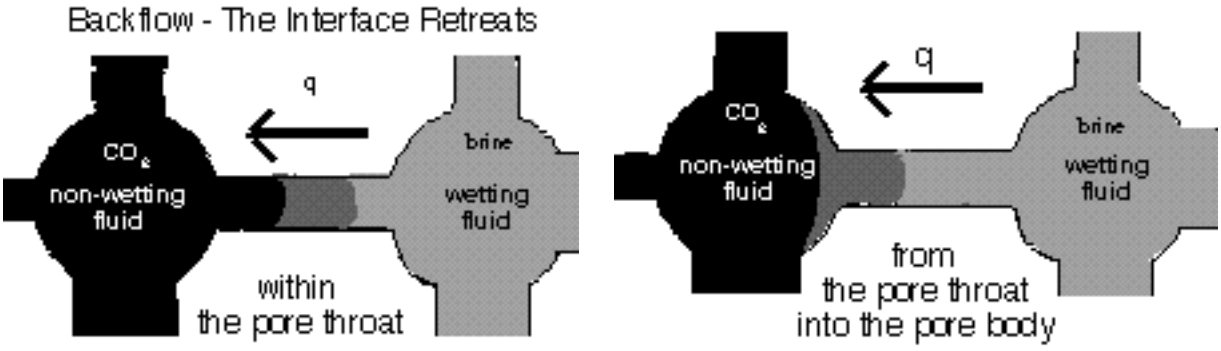

Figure 4 the CO_2 can retreat within the pore throat (left-hand figure) or through the pore throat into the pore body (right-hand figure).

We have attempted to make the flow-rules as non-restrictive and physical as possible.

i) All parts of the porous medium, pore-throats and pore-bodies have a volume which can be occupied by either type of fluid.

ii) Locally, back-flow as well as forward flow are allowed if they are ordained by the local pressure drops.

iii) Complications, such as over-filled pore bodies or plugs of fluid trapped in the pore throats are treated as physically as possible.

iv) Unphysical aspects, such as isolated 'blobs' of wetting fluids residing in pore-bodies, are tracked by the program and found to be insignificant.

v) Most importantly, the flow rules accurately account for all of the non-wetting fluid injected into the porous medium. For the smallest capillary number, there is a 0.25% difference between flow-rule

determination of the volume of injected fluid occupying the medium and the volume of fluid injected into or displaced out of the medium. For the larger capillary number, this difference is less than 0.01%.

IV. Results - Dependence of Saturations and Fingering Patterns upon N_c and M

In this section, we present results from running our computer code on systems which are 90 pores wide by 30 long (in the direction of average flow) using typical experimental values for surface tension and viscosity of CO_2 and brine as discussed in section II. We chose to model our flow on short wide systems, since long narrow geometries are known to mis-represent the fingering because of coarsening.[7]-[9] Figure 5 shows some typical, near-breakthrough fingering patterns where the CO_2 is injected along the lower edge.

Figure 6 shows near-breakthrough CO_2 saturation profiles for a wide range of capillary numbers with viscosity ratio M=0.05. The data points show averages over 5 different realizations of the porous medium (i.e. for each realization a different seed was used in the random number generator to determine the cross-sectional area of each throat); the error bars show the standard errors from the set of five realizations. Over this wide-range of capillary numbers there is little difference between the saturation profiles or between the total breakthrough saturations of CO_2 which are all around 20% or less.

Although the effect of capillary number on CO_2 saturation is small, if not negligible, capillary number has a significant effect upon the geometry of the fingering. For M=0.05, Figure 5a shows that the fingering for a low capillary number, $N_c = 6.25 \times 10^{-6}$, is identical to the fingering for IPwt (Invasion Percolation with trapping). Using the same model porous medium, the CO_2 occupation from our model for this low capillary number is shown by the open circles, while the CO_2 occupation from the IPwt is given by the small filled circles. That is, when the pore body location is marked by an open circle with a small filled circle inside, that same pore body was occupied by CO_2 using our model and independently by CO_2 using IPwt. For the five model porous media on which we've run the model, the agreement between IPwt and the model was excellent. In the worst case, the occupation of seven pore bodies was different between our model and IPwt. For the model porous medium shown in Fig. 5, the CO_2 occupation from the model and IPwt are identical. Figure 5b shows the CO_2 occupation at a larger capillary number for this same porous medium. Of course, since this is the same porous medium as that shown in Fig. (5a), the IPwt occupation, shown by the small filled circles, is the same for both. However, the fingering from the model at this large capillary number is very different from the IPwt fingering in Fig.5a. Indeed, at large capillary number the fingering from the model (open circles) is visually similar to DLA fingering.[7]-[9],[22] Since both DLA and IPwt have low breakthrough saturations, both of these fingering patterns are consistent with the CO_2 saturation profiles in figure 6.

These low CO_2 saturations for M=0.05 are to be contrasted with the saturations that can be achieved at larger viscosity ratios. For the same capillary numbers (i.e. the same surface tension and volume flows), we have performed the simulations with viscosity ratio, M=1. The

Figure 5 shows the occupation of a particular realization of a model porous medium.

The small solid circles show the CO_2 occupation as predicted by Invasion Percolation with trapping (IPwt).

The open circles show the CO_2 occupation as predicted by our pore-level model for M=0.05 and M=1 at two different Capillary numbers

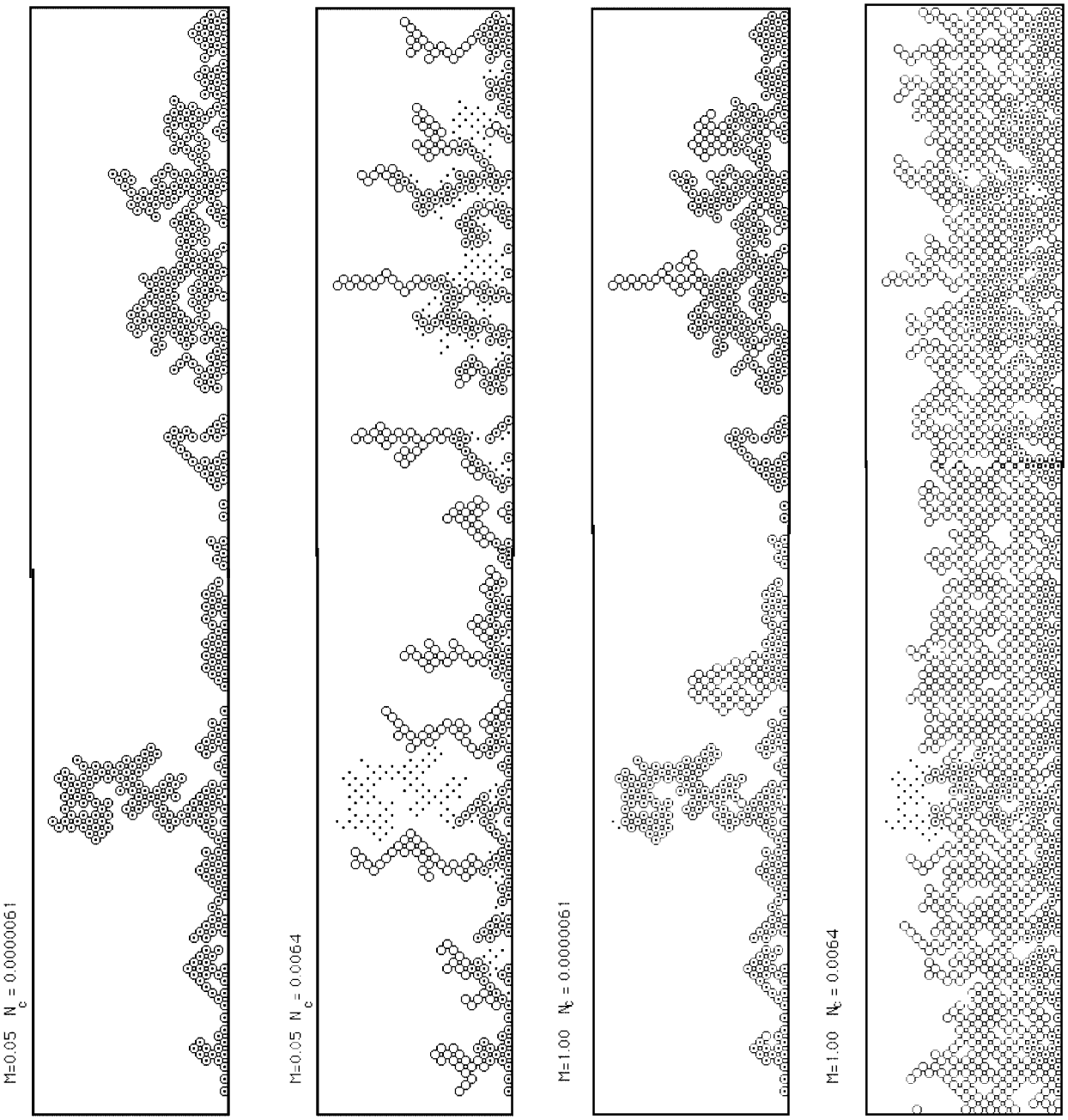

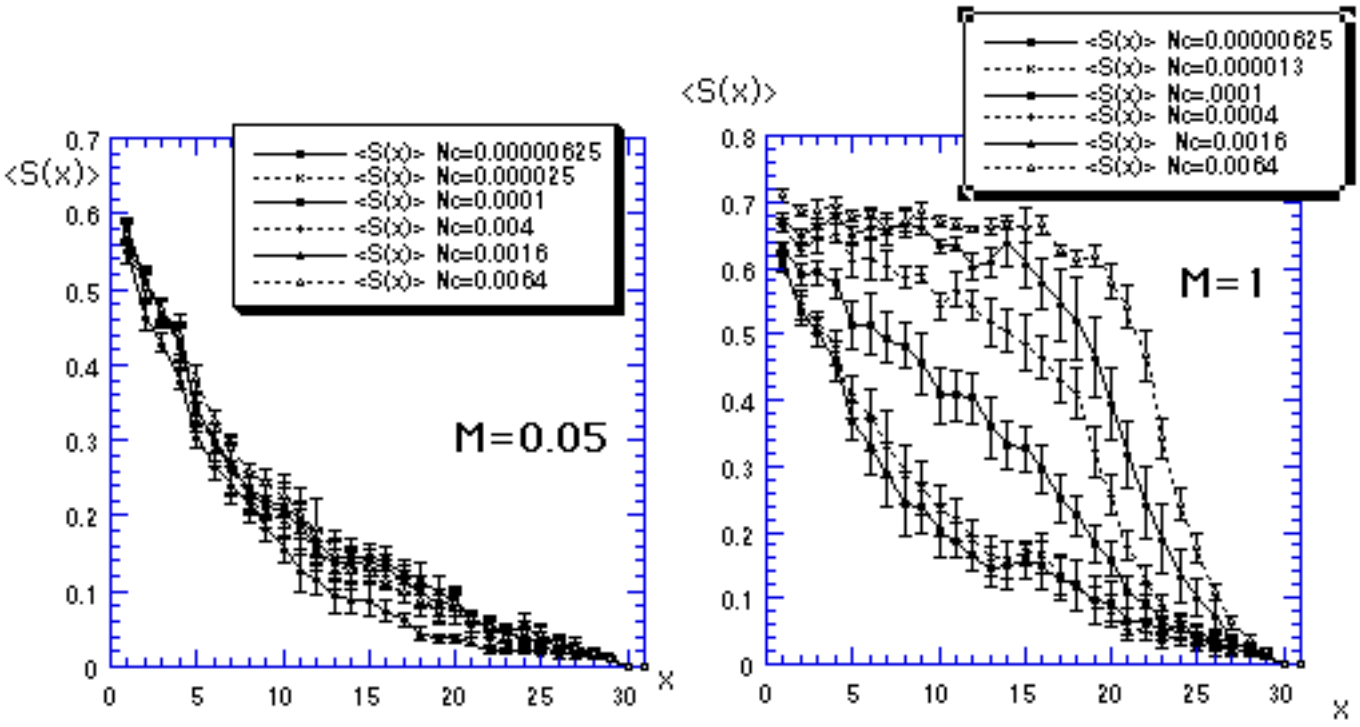

Figure 6 shows the near-breakthrough CO_2 saturation profiles of for viscosity ratios M=0.05 (left-hand figure) and M=1.00 (right hand figure) for a range of N_c from 6.25×10^{-6} to 6.4×10^{-3} .

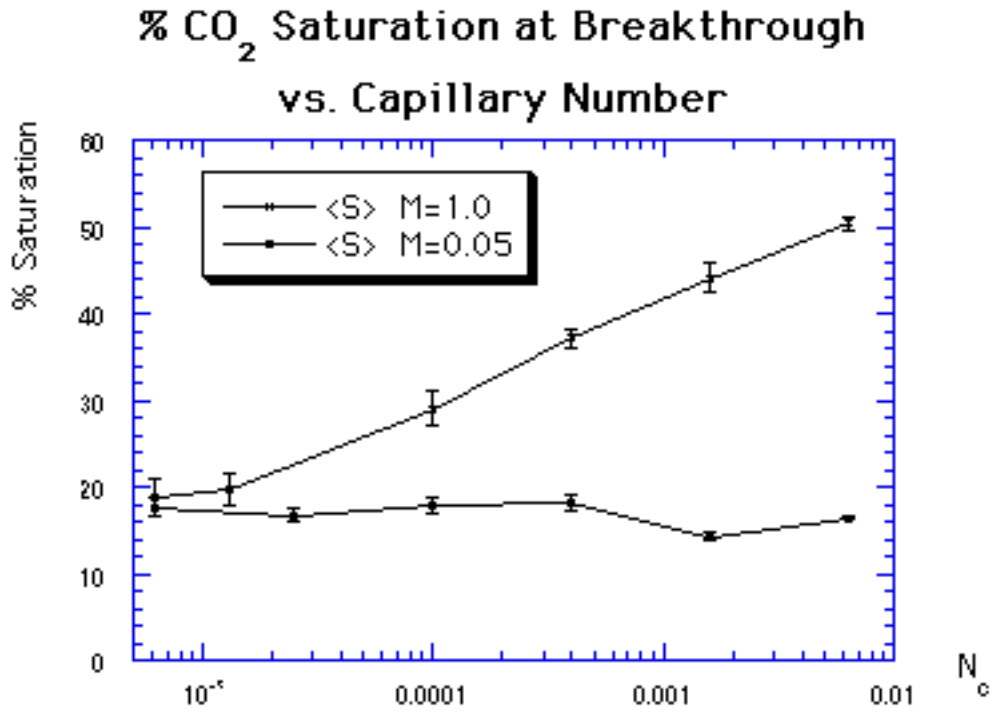

Figure 7 shows the breakthrough saturations of CO_2 in the 30x90 porous media with viscosity ratios M=0.05 (filled circles) and M=1 (x).

results are very different. At small capillary number, the M=1 saturations and fingering are similar to IPwt as they should be (see fig. 5c), but for M=1, even at this low capillary number deviations from IPwt are setting in. However, as capillary number increases, the flows become compact with negligible fingering (Fig. 5d) and the saturations increase dramatically (Fig. 6). Figure 7 shows the variation in CO_2 saturations at breakthrough vs. capillary number for both M=0.05 and M=1.00. As we've seen above, the breakthrough CO_2 saturations are nearly constant for M=0.05, whereas they increase significantly for the larger viscosity ratio M=1.0 .

V. Conclusions and Future Work

Our results from simulations show that injection of low viscosity CO_2 into the two-dimensional porous medium leads to small fractional saturations at breakthrough yielding the sequestration of only a small amount of carbon dioxide. If the viscosity of the carbon dioxide could be increased sufficiently, these results suggest that the efficiency of carbon dioxide sequestration could be doubled. Since this work has been done on small systems with only two viscosity ratios, it is important to ascertain how these effects change when one scales-up to realistically sized systems. However, it is interesting that the viscosity ratio M=0.05 produces DLA-like fingering on the size scale in Fig. 5, since our earlier work on miscible systems showed that flows for even smaller viscosity ratios were compact (negligible fingering) at even smaller size scales. It is also important to determine how this effect depends upon viscosity ratio throughout the range of physical interest.

References

1. Blackwell, R. J., J. R. Rayne and W. M. Terry, Trans. AIME, **216**, 1-8, (1959).
2. Collins, R. E., "Flow of Fluids through Porous Materials," 1961 Reinhold Publishing Corporation, New York.
3. Bear, J., "Hydraulics of Ground Water," 1979 McGraw-Hill Publ. Co., New York.
4. Dullien, F. A. L. "Porous Media: Fluid Transport and Pore Structure" 1979 Academic Press, New York.
5. Rhee, H.-K., R. Aris and N. R. Amundson, "1st-Order Partial Differential Equations: Vol. I (Theory and Applications of Single Equations," 1986 Prentice Hall, Englewood Cliffs, New Jersey.
6. Lenormand, R., E. Touboul and C. Zarcone, J. Fluid Mech., **189**, 165-187, (1988).
7. Feder, J., "Fractals," 1988 Plenum Press, New York.
8. Vicsek, T., "Fractal Growth Phenomena," 1989 World Scientific, Singapore.
9. Meakin, P., "Fractals, scaling, and growth far from equilibrium," 1998 Cambridge University Press, Cambridge.
10. Chen, J.-D. and D. Wilkinson, Phys. Rev. Lett., **55**, 1892-1895, (1985).
11. Nittmann, J., G. Daccord and H. E. Stanley, Nature, **314**, 141-144, (1985).
12. Daccord, G., J. Nittmann and H. E. Stanley, Phys. Rev. Lett., **56**, 336, (1986).
13. Witten, T. A. J. and L. M. Sander, Phys. Rev. Lett., **47**, 1400-1403, (1981).
14. Paterson, L., Phys. Rev. Lett., **52**, 1621-1624, (1984).

15. (Note the viscosity ration used in refs. 15-18 is the inverse of the one used in this paper.) Ferer, M. and D. H. Smith, Phys. Rev. E, **49**, 4114, (1994).
16. Ferer, M., R. A. Geisbrecht, W. N. Sams and D. Smith, Phys. Rev. A, **45**, 6973, (1992).
17. Ferer, M., W. N. Sams, R. A. Geisbrecht and D. H. Smith, AIChE J., **49**, 749, (1995).
18. Ferer, M., J. Gump and D. H. Smith, Phys. Rev. E, **53**, 2502-2508, (1996).
19. Halsey, T. C., P.Today DLA: A Model for Pattern formation, November, 36-41 (2000).
20. Wilkinson, D. and J. F. Willemsen, J. Phys. A, **16**, 3365, (1983).
21. Maloy, K., F. Boger, F. J and T. Jossang,Dynamics and Structure of Viscous Fingers in Porous Media,111-138,"Time Dependent Effects in Disordered Materials" , edited by Pynn and Riste (ed. 1987, Plenum Press, New York).
22. Ferer, M., G. S. Bromhal and D. H. Smith, Groundwater, to be sumbitted, (2001).
23. Vesovic, V. and e. al., J. Phys. Chem. Ref. Data, **19**, 763-808, (1990).
24. Chun, B.-S. and G. T. Wilkinson, Ind. Eng. Chem. Res., **34**, 4371-4377, (1995).
25. van der Marck, S. C., T. Matsuura and J. Glas, Phys. Rev. E, **56**, 5675-5687, (1997).
26. Aker, E. V K. Jorgen-Maloy ,A. Hansen and GT. Batrouni, Transport in Porous Media, **32**, 163-186, (1998).
27. Aker, E., K. Jorgen-Maloy and A. Hansen, Phys. Rev. E, **58**, 2217-2226, (1998).
28. Aker, E., K. Jorgen-Maloy and A. Hansen, Phys. Rev. E, **61**, 2936-2946, (2000).
29. Pereira, G., Phys. Rev. E, **59**, 4229-4242, (1999).
30. Akers, E., A Simulation for Two-Phase Flow in Porous Media, (1996).